J. Biophotonics **10**, 1110–1114 (2017) / **DOI** 10.1002/jbio.201600320

Journal of BIOPHOTONICS

LETTER

Diffractive corneal inlay for presbyopia

Walter D. Furlan,*[,1] *Salvador García-Delpech*,[2] *Patricia Udaondo*,[2] *Laura Remón*,[3] *Vicente Ferrando*,[4] *and Juan A. Monsoriu*[4]

[1] Departmento de Óptica y Optometría y Ciencias de la Visión, Universitat de València, 46100, Spain
[2] Ophthalmology Department, Hospital Universitario La Fe, Valencia, 46026, Spain
[3] Departamento de Física Aplicada, Universidad de Zaragoza, España
[4] Centro de Tecnologías Físicas, Universitat Politècnica de València, Valencia, 46022, Spain

Received 18 December 2016, revised 13 April 2017, accepted 27 April 2017

Keywords: Presbyopia, refractive surgery, cornea, diffractive lenses

A conceptually new type of corneal inlays for a customized treatment of presbyopia is presented. The diffractive inlay consists on a small aperture disc having an array of micro-holes distributed inside the open zones of a Fresnel zone plate. In this way, the central hole of the disc lets pass the zero order diffraction and produces an extension of the depth of far focus of the eye, while the diffracted light through the holes in the periphery produce the near focus. Additionally, the micro-holes in the inlay surface fulfill the essential requirement of allowing the flow of nutrients through it to the cells of the corneal stroma. Theoretical and optical-bench experimental results for the polychromatic axial Point Spread Function (PSF) were obtained, showing an improved performance compared to the small aperture corneal inlay currently in the market (Kamra). Images of a test object, obtained at several vergences in the surroundings of the far and near foci, are also shown.
Picture: Simulation of the appearance of the Diffractive corneal inlay on a real eye.

1. Introduction

The treatment of presbyopia has been historically addressed from different perspectives: from spectacles and contact lenses [1], to surgical approaches [2]. The most recent alternative is the use of intracorneal implants, also known as corneal inlays. According to their physical properties, this type of implants can be divided in two main groups. On the one hand, refractive inlays are intended to locally modify the power of the cornea by changing either, the refractive index, or its curvature [2]. On the other hand, the small aperture corneal inlay, commercially known as Kamra™ (AcuFocus, Irvine, CA, USA), is based on the pinhole effect, thanks to which it is possible to increase the depth of focus (DOF) of the eye, providing good vision at intermediate and short distances. The Kamra inlay is an opaque (black) thin ring of polyvinylidene fluoride (PVDF) with 3.8 mm diameter and a central aperture of 1.6 mm [2,3]. It has 8,400 micro-holes (of 5–11 μm diameter) randomly distributed in its

* Corresponding author: e-mail: walter.furlan@uv.es

surface for facilitating the flow of nutrients to the cells of the corneal stroma. With these dimensions, the Kamra let pass through the central hole only about 20 % of the light that reaches it, and around 5 % is diffracted through the permeable material. Therefore, it is implanted only in one eye (monovision). In spite of the good clinical outcomes, the small aperture inlay has some shortcomings. A significant reduction in the contrast sensitivity of the surgical eye has been reported [3]; which is caused by the combination of the small aperture (pinhole effect) and the diffracted light by the micro-holes in the opaque ring. Additionally, under low illumination, the use of a small aperture inlay could make reading difficult, and also can cause problems in stereoscopic acuity due to the differences between the luminance of retinal images [4,5].

In this letter we present a conceptually new amplitude corneal inlay, with improved light throughput. This Diffractive Corneal Inlay (DCI), in addition to produce an extension of the depth for the far focus of the eye, it creates a near focus taking advantage to the light diffracted by the nutrient micro-holes in its surface. Numerical simulations of the axial PSF are presented for different pupil diameters. The improved focusing and imaging performance of the DCI is demonstrated with experiments performed under polychromatic illumination in an optical bench.

2. Diffractive inlay design

The main idea behind the design of the DCI is to exploit the intrinsic diffraction produced by the nutrient-permeable micro holes, redistributing them in annular zones that coincide with those of an amplitude Fresnel zone plate (see Figure 1a), to create a diffractive lens. A similar concept, called photon sieve, was proposed formerly by Kipp et al. [6] for focusing X-rays.

A photon sieve is in fact a variation on the Fresnel zone plate, which instead of alternate transparent and opaque rings of equal area, is an opaque disc with non-overlapping pinholes distributed in the corresponding transparent Fresnel zones. It was reported that photon sieves can achieve a sharper focus by suppressing the secondary maxima and higher-order diffraction effects as compared to a Fresnel zone plate [6–9]. Accordingly, the diffractive corneal inlay (DCI) here proposed, is a single micro-structured device (with any substrate) that combines the concepts of small aperture inlay and photon sieve. Therefore, a DCI has two main foci: one, the far distance focus, which is formed mainly by the light that passes through the central hole; and the other one, the near distance focus, that is generated

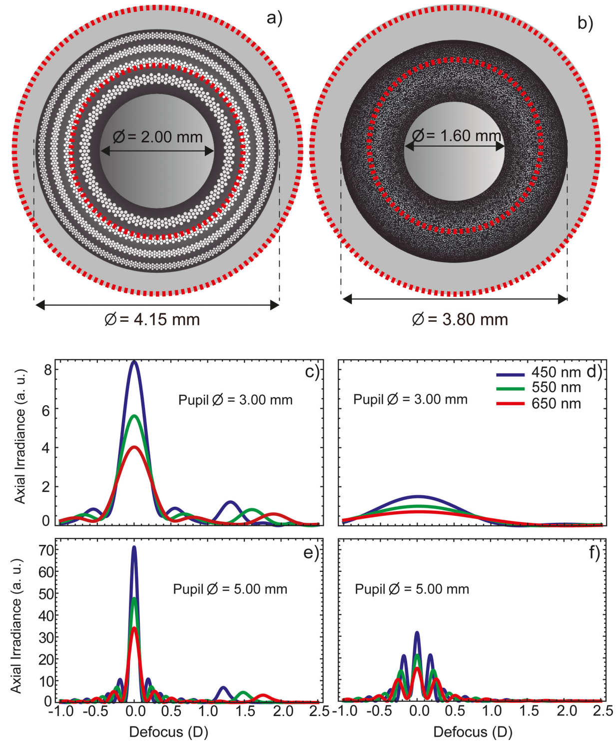

Figure 1 a) Diffractive Corneal Inlay (DCI) (see the main text for details of design parameters); b) Small aperture inlay with the dimensions of the Kamra. Dashed red lines in a) and b) represent the 3 and 5 mm diameter pupil. c) Monochromatic theoretical axial PSFs for 45 nm (blue line), 550 nm (green line) and 650 nm (red line) computed for a 3 mm pupil diameter (c) and 5 pupil diameter (e). d) and f) Idem c) and d) but computed for the small aperture inlay.

by the light diffracted by the micro-holes in the annuli (first diffraction order). Hence, the effects of the high diffraction orders on the far and near images are minimized, because of the destructive interferences produced by the spatial distribution of the micro-holes [6,9]. Moreover, the spatial distribution and diameter of micro-holes in each zone can also be modified to obtain an optimized relative intensity between the near and far foci, and/or to correct high order ocular aberrations. A typical example of a DCI is shown in Figure 1a. The construction parameters are listed in Table 1, in comparison with the only small aperture inlay available on the market: the Kamra, shown Figure 1b.

As can be noted, in this particular example the distribution of the micro-holes in Figure 1a alternates an azimuthal sequence of two and three holes per zone.

To evaluate the focusing properties of the DCI we have computed the axial irradiance provided by

Journal of
BIOPHOTONICS

Table 1 DCI and Kamara corneal inlays construction parameters.

	Design wavelength	Addition (Ad)	Central hole diameter	External diameter	Total number of holes	Maximum hole diameter	Minimum hole diameter
DCI	550 nm	1.50 D	2.00 mm	4.15 mm	2,290	30.5 μm	18.8 μm
KAMRA	550 nm	NA	1.60 mm	3.80 mm	8,400	11 μm	5 μm

both devices under plane wave coherent illumination. By using the Fresnel approximation, we numerically computed monochromatic irradiances for different wavelengths [10] and two pupil diameters: 3.00 mm and 5.00 mm. These pupils diameters were selected because they are representative for people from 40 to 60 years old, in bright and dim environments respectively [11] and also because they were adopted in other studies dealing with Kamra [12]. The results are shown in Figures 1c–1f. As expected, the diffracted intensities are wavelength-dependent with maximum irradiances for the design wavelength. As can be noted in Figures 1e and 1f, the 5.00 mm pupil allows the light to pass outside the inlays increasing the values of the axial intensity, and creating an interference pattern along the optical axis. Note that, for each pupil diameter, the same normalization was adopted to represent the results provided by both inlays, and, therefore, the relative intensity values can be directly compared. This particular example was aimed to show the diffractive behavior of the DCI. A more realistic comparison has been performed with incoherent polychromatic light as follows.

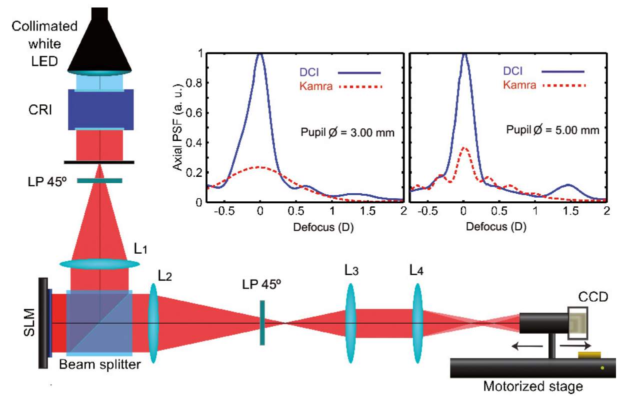

Figure 2 Scheme of the experimental setup employed to obtain the polychromatic axial PSF.A 30 μm pin-hole (PH) acts as a point object. LP 45° are linear polarizers to allow the system to work in amplitude-only mode. L1 and L2 are achromatic lenses of 200 mm focal length. L3 and L4 are achromatic lenses of 100 mm focal length. The experimental axial illuminances (polychromatic through the focus PSF) for the DCI (continuous blue line) and for the small aperture inlay with the dimensions of the Kamra (dashed red line) are represented in the upper right corner for two different pupil diameters.

3. Experimental results

We have experimentally tested the focusing properties of our DCI, described in the previous section. To do that, we employed an optical bench testing method based on the use of a Liquid Crystal Spatial Light Modulator (SLM). The system, shown in Figure 2, provides the polychromatic through-focus PSF of the lens under test in a totally automated procedure A detailed description of the experimental setup can be found elsewhere [8]. The DCI, and an opaque annulus with the dimensions of the Kamra inlay (with no microholes) were replicated on a Liquid Crystal in a Silicon SLM (Holoeye PLUTO, 8-bit gray-level, pixel size 8 μm, and resolution 1920 × 1080 pixels), operating in amplitude mode, and calibrated for different wavelengths in the visible range. The illumination system consisted of a Cold-White collimated LED (Mounted High-Power LED, CW, 1000 mA) and CRI VariSpec Liquid Crystal Tunable Filter. This filter allows us to select a wavelength in the visible range with a bandwidth of 10 nm. A pinhole (PH) with a diameter of 30 μm (the point-like object) was located at the focal plane of an achromatic lens L1. A parallel light beam was directed to a beam splitter that reflects it to the SLM, where the inlays shown in Figure. 1a and Figure. 1b were simulated. Then, using a 4f setup, the images of the inlays were projected onto a 10.0D achromatic lens, L4, acting as artificial cornea. Finally, the through the focus PSFs were captured along the optical axis and registered with a CCD camera (12 bit gray-level, pixel pitch of 3.75 μm, and 1280 × 960 pixels) mounted on a translation stage (Thorlabs LTS 300). Images for 54 wavelengths of visible light (450 nm–720 nm). were captured at 120 axial positions, covering object vergences in the range −0.75 D to +2.0 D. Then the polychromatic PSF along the optical axis was computed in terms of the CIE Tristimulus values: $X(\lambda)$ $Y(\lambda)$, $Z(\lambda)$ [14]; in particular as the axial illuminance defined as:

$$Y(\lambda) = \int_{\lambda_1}^{\lambda_2} I(z;\lambda)\, S(\lambda)\, y(\lambda)\, d\lambda \tag{1}$$

where $y(\lambda)$ is the corresponding the spectral sensitivity curve of the CIE standard observer; (λ_1, λ_2) represents the considered wavelength interval; $S(\lambda)$, is the spectral power distribution of the light source (the CIE illuminant C), and $I(z;\ \lambda)$ are the experimental values of the irradiances obtained along the optical axis z. Figure 2 shows the resulting axial polychromatic PSFs. Note that the experimental results of the axial illuminance agree very well with the expected results from the monochromatic theoretical irradiances shown in Figure 1. An improved performance of the DCI against the Kamra in almost the whole range of vergences can be clearly seen, particularly at the near and far foci. As expected, the contrast of the near image is affected by the light coming from the far focus, and also, by the inevitable first negative (virtual) diffraction order focus.

We have also tested the image forming capabilities of DCI under white-light illumination. In this case the pinhole in the experimental setup was replaced by a binary object-test (the acronym of our group). Figure 3 shows the images transformed to RGB coordinates [9]. provided by the DCI, at the main focal planes. To obtain defocused images, the image plane was axially displaced in steps of 0.25 D around the focal planes.

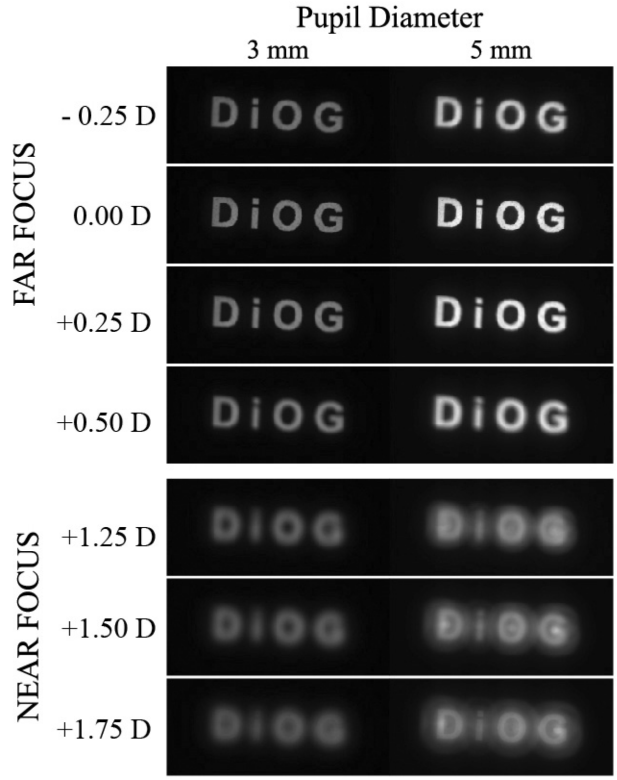

Figure 3 Polychromatic images of a test object obtained with the DCI around the far and near foci for two different pupil diameters.

4. Conclusion

A new concept of amplitude corneal inlay for the treatment of presbyopia has been presented and tested in an optical bench. The inlay consists on an opaque ring, in which the micro-perforations that are needed to nourish the corneal tissue are arranged to conform a diffractive lens. Hence, the intrinsic and undesired diffractive effects produced by the microholes in the conventional small aperture inlay are turned into an advantage in our design, for creating a true near focus. Compared with the current small aperture inlay in the market, significant improvement in the axial irradiance has been demonstrated.

It is very important to note that our proposal is feasible with the present technology since the manufacturing materials and methods can be the same as those used to construct the Kamra. Advantageously, the design parameters of the DCI allow customization, which is a new concept in corneal implants. In fact, the DCI can be designed to match the patient's addition (which evidently can be different from the 1.5 D add, here reported as an example), pupil diameter, and visual needs. In particular, the ratio between the near and far intensities can be modified by varying the ratio between the clear and opaque areas in each Fresnel zone of the inlay [15], the inlay inner and outer radii, and the number and density of holes.

According to the results presented in Figure 2, some small residual myopia might be required to even improve optical outcomes with the DCI, as was also reported for the Kamra inlay [16].

The effect of mutual disturbance between the near and far foci has been demonstrated to be harmless compared to the improvement in both far and near vision in scotopic conditions (see Figure 3). The longitudinal chromatic aberration of the near focus is opposed in sign to that of the eye (see Figure 1c–e), so, it is expected to be partially compensated in real eyes [17].

Further studies are required to investigate this effect and others like, decentrations. Previous studies with the Kamra show that, this inlay is very sensitive to decentration [3]. Nevertheless, its good clinical outcomes confirm that surgical skills and techniques, can overcome this problem. Other potential side effect that was found in other corneal inlays, is the loss of transparency after several months of the surgery. However, in a recent study, Alio et al. [18] reported that, in just two of ten patients that needed Kamra's removal (from a total of 135 surgeries), slit lamp examination revealed that only mild haze was noted at six months after removal. Consequently, in spite of being something premature at this stage, we have a basis to expect the same good results for the DCI. The binocular effect of the DCI will also be addressed in the future. In fact, due to its high efficiency, compared with the Kamra, the DCI could be implanted in both eyes without creating problems of binocular vision. Moreover, since the surgery is limited to the cornea, it would be safer than other intraocular surgeries for correction of presbyopia, like phakic or pseudophakic intraocular lenses. It is also safer than LASIK as it does not remove any corneal tissue, thus minimizing the risk of ectasia. Nevertheless, in ametropic eyes the surgical procedure is fully compatible with LASIK and PRK to treat simultaneuously ametropia and presbyopia.

Acknowledgements This study was founded by Ministerio de Economía y Competitividad FEDER (Grant DPI2015-71256-R), and by Generalitat Valenciana (Grant PROMETEOII-2014-072), Spain.

Conflict of interest W.D. Furlan, S. García-Delpech, P. Udaondo, L. Remón, and J. A. Monsoriu have a patent "Lente ofttálmica para la correción de la presbicia" issued. V. Ferrando report no conflicts of interest and have no proprietary interest in any of the materials mentioned in this article.

References

[1] W. N. Charman, Ophthalmic Physiol Opt. **34**, 8 (2014).
[2] W. N. Charman, Ophthalmic Physiol Opt. **34**, 397 (2014).
[3] O. Seyeddain, A. Bachernegg, W. Riha. T. Rückl, H. Reitsamer, G. Grabner, and A. K. Dexl, J Cataract Refract Surg. **39**, 234 (2013).
[4] J. Tabernero, C. Schwarz, E. J. Fernández, and P. Artal, Invest Ophthalmol Vis Sci. **52**, 5273 (2011).
[5] S. Plainis, D. Petratou, T. Giannakopoulou, H. Radhakrishnan, I. G. Pallikaris, and W.N. Charman, PLoS One **14**, 8(10) (2013).
[6] L. Kipp, M. Skibowski, R.L. Johnson, R Berndt, R. Adelung, S. Harm, and R. Seemann, Nature **414**, 184 (2001).
[7] R. Menon, D. Gil, J G Barbastathis, and H. Smith, J. Opt. Soc. Am. A **22**, 342, (2005).
[8] G. Andersen, Appl. Opt. **49**, 6391 (2010).
[9] F. Giménez F, J.A. Monsoriu, W.D. Furlan, and A. Pons, Opt Express **14**, 11958 (2006).
[10] F. Giménez, W. D. Furlan, A. Calatayud, and J. A. Monsoriu, J. Opt. Soc. Am. A **27**, 1851 (2010).
[11] A. B. Watson, J.I. Yellott J. Vis. **12**, 1 (2012).
[12] C. Schwarz, S. Manzanera, P. M. Prieto, E. J. Fernández, and P. Artal, Biomed. Opt. Express **5**, 3355 (2014)
[13] V. Ferrando, F. Giménez, W. D. Furlan, and J. A. Monsoriu, Opt. Express **23**, 19846 (2015).
[14] D. Pascale, A Review of RGB Color Spaces. from xyY to RGB (The Babel Color Company, Montreal, Canadá (2003).
[15] D. C. O′Shea; T. J. Suleski; A. D. Kathman,. & D. W. Prather, Diffractive Optics: Design, Fabrication, and Test, Tutorial Texts in Optical Engineering Vol. TT62, SPIE Press, ISBN 0-8194-5171-1, Washington, USA (2004) Ch. 5 p. 86.
[16] J. Tabernero, P. Artal, J. Cataract. Ref. Surg. **38**, 270 (2012).
[17] P. Artal, S. Manzanera, P. Piers, and H. Weeber, Opt. Express **18**, 1637 (2010).
[18] J. L. Alio, A. Abbouda, S. Huseynli, et al., J. Refract. Surg. **29**, 550 (2013).